Pol. J. Environ. Stud. Vol. 31, No. 2 (2022), 1783-1790
DOI: *10.15244/pjoes/142609* ONLINE PUBLICATION DATE: 2022-01-25

Original Research

Shear Properties of Grout-Rock Interface for Treatment of Mud Inrush

Li Peng[1], Zhang Qingsong[2], Sun Lianyong[3], Huang Yongliang[3], Chen Xuguang[1]*, Wang Chengqian[1], He Lingyao[1]

[1]Engineering College, Ocean University of China, Qingdao, 266100, China
[2]Geotechnical and Structural Engineering Research Center, Shandong University, Jinan, 250061, China
[3]Ji'nan Rail Transit Group Construction Investment Co., Ltd. Jinan, Shandong, 250000, China

Received: 26 July 2021
Accepted: 27 September 2021

Abstract

Grouting is an effective method to strengthen weak rock mass in tunnel engineering to prevent and control mud inrush disaster. The hardened grout-rock consolidation involves not only the properties of hardened grout, but also that of weak rock masses. As a transition region between them, the grout-rock interface determines the overall strength, then the shear properties of which was investigated in this study. The gushed mud from engineering project and a kind of Portland cement grout were selected as raw materials. A test system that can apply high injection pressure was developed to simulate the actual generation environment of grout-rock interface. By using it, two sets of samples with three different water-to-cement (W/C) ratios: 0.8, 1 and 1.5; and three different injection pressures: 1 MPa, 1.5 MPa and 2 MPa were prepared. After that, the direct shear test and SEM test were conducted to study the properties of grout-rock interface. The results show that lower W/C ratio and higher injection pressure can result in larger cohesive strength as well as internal friction angle of samples. When W/C ratio was decreased from 1.5 to 0.8, the former increased from 171.95 kPa to 251.55 kPa, and the latter rose from 32.31° to 41.71°. Also, they increased by 73.59 % and 17.64 %, respectively, with injection pressure ranging from 1 MPa to 2 MPa. It is hoped that the data provided will aid in the design of grouting with this material in the future.

Keywords: mud inrush, grout-rock interface, shear properties, hardened grout

Introduction

The large-scale tunnel construction in China is developing rapidly, and the tunnel excavation usually exposes unfavorable geology, e.g. weak rock masses, which is easy to induce mud inrush, and then it will result in irreversible damage to the environment [1-3]. To deal with it, the grouting method, in terms of fracturing grouting, permeation grouting, filling grouting and compaction grouting, has been widely used to enhance the mechanical properties of weak rock masses in tunneling engineering [4, 5]. Among them, fracturing grouting will be the dominant process [6], when grout injections are conducted in the ground with low permeability, such as soil. Driven by high pressure,

*e-mail: chenxuguang1984@ouc.edu.cn

grouts are injected into ground to create fractures [7], and then to densify and combine with ground. In this way, the strength of ground can be improved. Therefore, one of the core issues in grouting applications is to select suitable grouting material [8]. Because of high strength, good injectability, excellent durability and low cost, the cement-based grout has become the most commonly used grouting material in the past decades [9].

In order to assist in assessing the effectiveness of this ground treatment, the properties of cement-based grout has been one of the most interesting areas of research in grouting materials. For example, Varga et al. evaluated the grout-concrete interface bond performance by performing a dimensional stability study [10]. Chen et al. conducted triaxial tests to investigate the shear behaviors of a modified Portland cement grout with two different water-to-cement (W/C) ratios [11]. In the shape of small scale cylinders, Jorne et al. studied the injectability of grouts in 11 kinds of porous media with different characteristics along the height of injection [12]. Li et al. measured the rheological and mechanical properties of 6 kinds of MC grouts, and 2 kinds of ordinary Portland cements [13]. Although all these studies mentioned above contribute to better understand the properties of cement-based grout, they only focused on the grout itself, including bond performance, shear behaviors, injectability, rheological and mechanical properties.

As a matter of fact, the ground improvement involves not only the properties of grout, but also that of weak rock masses. That's to say, it is the strength of combination of hardened grout and weak rock masses that directly determines the effectiveness of this ground treatment. In this regard, Shahu et al. studied the fly ash content, dolime content, and curing period on the shear strength of copper slag-fly ash-dolime mix [14]. Yang et al. investigated the effect of cement content on shear strength of soil-cement [15]. However, a variety of materials were mixed together under no pressure, which is different from grouting process with high injection pressure. Salimian et al., Hu et al. and Han et al. experimentally investigated the mechanical properties of fractured rock masses both before and after grout injection [16-18], respectively. They innovatively studied the strength of combination of hardened grout and weak rock masses, however, as a combination, the transition region between two materials was ignored.

Zhang et al. conducted a series of grouting simulation tests in soil to study the strength improvement caused by grouting [19]. Specifically, based on the results of uniaxial compression tests, it was reported that the strength of combination of hardened grout and soil can increase by 181 % to 2535 % after grouting. Meanwhile, it was found that the interfaces between hardened grout and weak rock masses (grout-rock interface) controlled the compression failure process of specimens. This is mainly because that the hardened grout and rock masses have obviously different mechanical properties, and then they tend to show inconsistent deformation characteristics when stressed. Thus, as a transition region between hardened grout and rock masses, it's the interface that determines the overall strength. The issue of interface properties should therefore receive considerable critical attention.

In order to overcome the aforementioned problems, this study focuses on the shear properties of grout-rock interface. First, a test system that can apply high injection pressure was developed to simulate the actual generation environment of grout-rock interface. Then, two sets of samples with three different water-to-cement (W/C) ratios and three different injection pressures were prepared.

Material and Methods

Raw Materials

Yonglian tunnel, located on highway from Ji'an City to Lian'hua City, in Jiangxi Province, China, suffered multiple accidents such as collapse and mud inrush during the construction process [20, 21]. The tunnel runs through a total of three faults, one of which is the main cause of geological disasters, then this fault was named fault-2, which is composed of highly weathered sandstone and shale with extremely low strength and permeability. Due to high content of montmorillonite, it can turn into gushed mud under the action of water. With the plasticity index of 22.3, the gushed mud can be classified as clay with small particle size. When grouting method was used to improve the properties of surrounding rock, it was found that the kind of fracturing grouting was the dominant process, furthermore, there were obvious interfaces between grouts and weak rock masses. Thus, the gushed mud in Yonglian tunnel was selected as a representative of weak rock masses in this study, with the optimum moisture content of 23.1 % and the maximum dry density of 1700 $kg \cdot m^{-3}$. Furthermore, according to the soil test results, its liquid limit and plastic limit can reach 48.3 % and 25.6 % [22], respectively. A kind of ordinary Portland cement grout, produced by Sunnsy Group, is selected in this study. This is because it has been widely used in grouting engineering, also in Yonglian tunnel.

Sample Preparation

A well-known fact is that grout is usually injected into weak rock masses in the high injection pressure condition in practice [23, 24], thus the process of sample preparation should be under similar condition. To realize it, a test system consisting of cylindrical grouting device and parameter-controlled grout pumping equipment, was developed. As shown in Fig. 1, the cylindrical grouting device is made of high-strength steel, which has a high injection pressure bearing capacity. Then, six screws are designed to

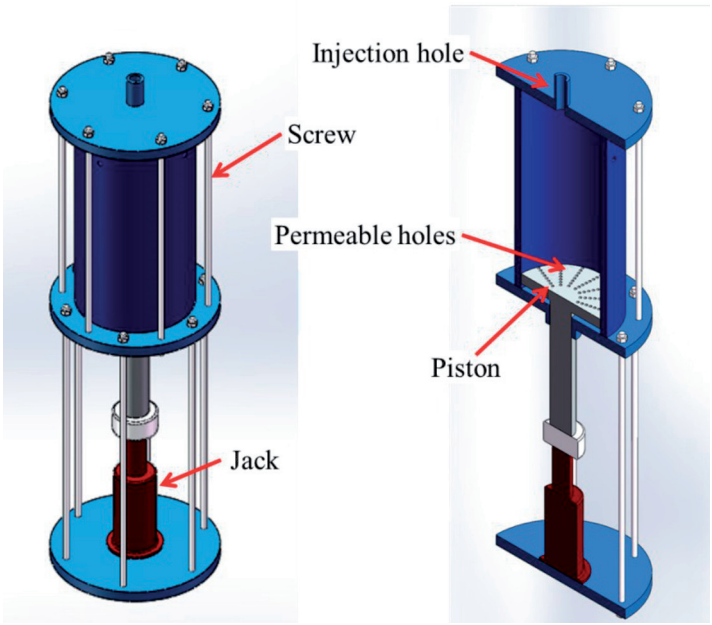

Fig. 1. Structure of cylindrical grouting device.

tighten the cylindrical grouting device. Furthermore, the rubber pads and glass glue were used to seal the contact surface between the cavity and the top plate. In this way, the cylindrical grouting device can realize grouting under high injection pressure conditions, which can be up to 3 MPa. On this basis, by adopting the same grouting materials, grouting technology and weak rock masses as engineering practice, the actual generation environment of grout-rock interface can be simulated. Fig. 1 illustrates the detailed structure of grouting device where gushed mud filling and grout injection conducted, with a height of 0.4 m and an inner diameter of 0.184 m.

In order to get flatter grout-rock interfaces, the structural planes with a thickness of 1×10^{-3} m to 2×10^{-3} m were preseted inside the samples before grouting, controlling the direction of fractures. The principle of determining the thickness of the structural planes is to reduce the disturbance of the soil and technical achievability. After grouting, the combination of hardened grout and gushed mud was firstly jacked out of cylindrical grouting device, as shown in Fig. 2, and the volume of injected grout varies from 2 L to 3 L. Then, the grout-rock interface samples were obtained by using cutting ring with an inner diameter of 6.18×10^{-2} m and a thickness of 2×10^{-2} m, and Fig. 3 presents the process of sample preparation. After that, the samples were cured in indoor temperature of around 20ºC for 7 days.

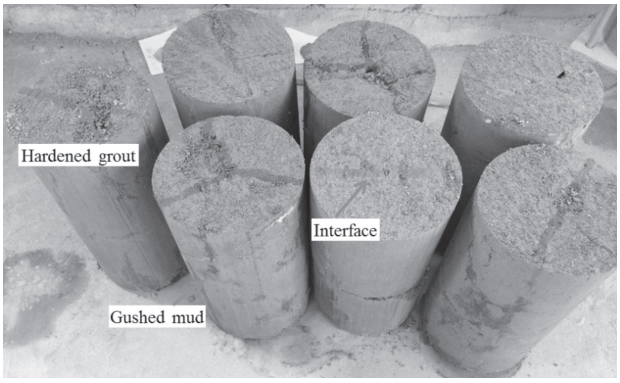

Fig. 2. Photo of samples after grouting.

Test Array

Previous studies show that injection pressure and water-to-cement (W/C) ratios are the two of the most important parameters of grouting [25], directly determining the mechanical properties improvement of weak rock masses. Therefore, this study focuses on the effect of the above-mentioned two factors on shear properties of grout-rock interface, and then two sets of grouting tests were arranged. Table 1 tabulates that three W/C ratios: 0.8, 1 and 1.5 were selected to prepare samples under the same injection pressure of 1 MPa. Similarly, three injection pressures: 1 MPa, 1.5 MPa and 2 MPa were applied during grout injection process under the same W/C ratio of 1.

Direct Shear Test

This study mainly focuses on the shear properties of grout-rock interface. A self-control direct shear apparatus, consisting of stepping motor, vertical force application device, force sensor, shear displacement sensor and data acquisition system, was developed to meet the requirements of carrying out a large number of shear tests, as shown in Fig. 4. This apparatus

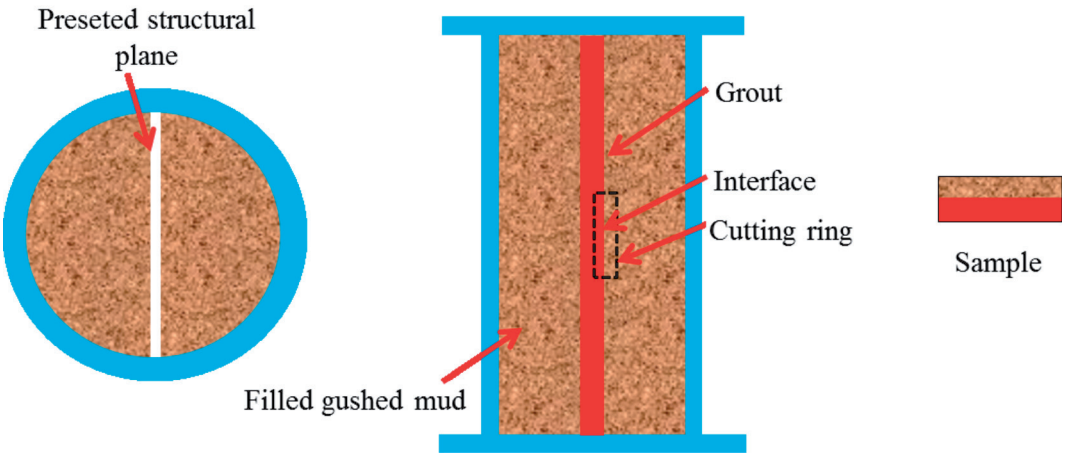

Fig. 3. Diagram of sample preparation process.

is able to realize that the shear rate ranges from 3.3×10^{-7} m/s to 4×10^{-5} m/s, and the maximum shear force can reach 5×10^{3} N. Furthermore, by using sensors and data acquisition system, the real-time shear stress-strain curves of samples can be recorded automatically during the test. Each test was replicated three times and the average values were selected as the final results.

Results and Discussion

Shear Properties of Grout-Rock Interface with Different W/C Ratios

During the test, the shear rate was kept a constant value of 1 mm/min. Fig. 5a) presents the shear stress-strain curves of sample 1 when a series of vertical stresses (σ): 100 kPa, 200 kPa, 300 kPa, and 400 kPa were applied. It can be seen that the stress increases rapidly with displacement in the initial stage until it reaches a maximum value. Then, there is a gradual decrease of the shear stress to a roughly stable residual value. Apparently, the samples generally show ductile behaviors in the shear process. Specifically, when the vertical stress is increased from 100 kPa to 400 kPa, the peak stresses can increase by 22.7%, 20.03% and 20.54%, respectively, with the corresponding displacements ranging from 1.67×10^{-3} m to 2.97×10^{-3} m. It can also be seen that the curves are not very regular. This is because the grout-rock interface may be not flat but curved, and not exactly coincident with the shear plane, that is to say, the grout-rock interface here actually refers to a bond zone, not a straight line. Thus, there may be small changes in the shear performance of sample along the shear path.

Using the same method, the shear stress-strain curves of sample 2 and sample 3 in different vertical stresses conditions were also acquired, as shown in Fig. 5b) and Fig. 5c). It can be found that the maximum stresses of the former are 301.65 kPa, 366.5 kPa, 440.37 kPa and 534.53 kPa, and that of the latter can reach 241.83 kPa, 388.4 kPa, 552.93 kPa and 752.17 kPa, respectively. Furthermore, both of them show the similar ductile behaviors to sample 1.

Based on the shear strength of grout-rock interface in different vertical stresses conditions, the Mohr-coulomb law was used to obtain the cohesive strength and internal friction angle [26], as tabulated in Table 2. Therefore, the direct shear strength of grout-rock interface with W/C ratios of 0.8, 1 and 1.5 can be expressed as Eq. (1), Eq. (2) and Eq. (3), respectively.

Table 1. Two sets of grouting tests.

Test array	Trial number	Injection pressure (MPa)	w/c ratio
First set	Sample 1	1	0.8
	Sample 2		1
	Sample 3		1.5
Second set	Sample 4	1	1
	Sample 5	1.5	
	Sample 6	2	

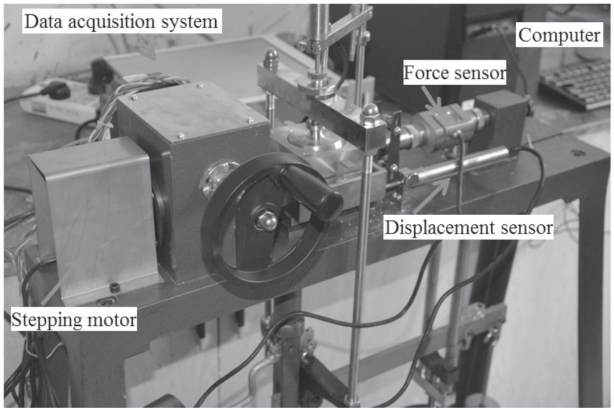

Fig. 4. Assembling of the self-control direct shear apparatus.

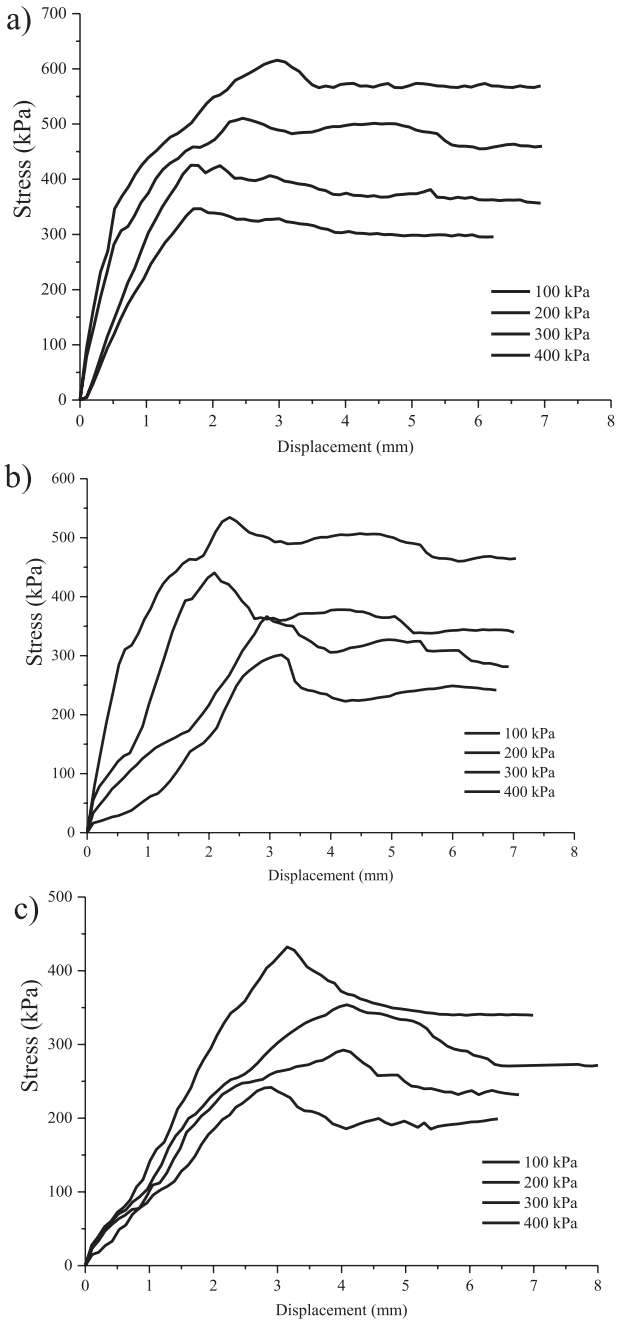

Fig. 5. Shear stress-strain curves of sample with different W/C ratios.

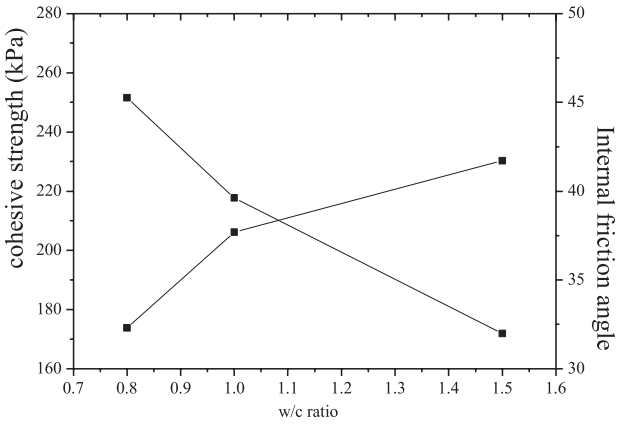

Fig. 6. Cohesive strength and internal friction angle of samples in different W/C ratio conditions.

$$\tau=0.89\sigma+251.55 \quad (1)$$

$$\tau=0.77\sigma+217.74 \quad (2)$$

$$\tau=0.63\sigma+171.95 \quad (3)$$

where, τ = shear strength of grout-rock interface, kPa; σ = vertical stress, kPa.

After that, the cohesive strength - W/C ratio relationship and internal friction angle - W/C ratio relationship were plotted as Fig. 6. It can be seen that when injection pressure was kept constant, the W/C ratio has a significant effect on both cohesive strength and internal friction angle of samples. Specifically, when W/C ratio decreased from 1.5 to 1, the cohesive strength increases from 171.95 kPa to 217.74 kPa, and the internal friction angle rises from 32.31° to 37.69°. Also, the cohesive strength and internal friction angle can increase by 15.53 % and 16.65 %, respectively, with W/C ratio ranging from 1 to 0.8. Thus, it can be concluded that low W/C ratio can significantly increase the cohesive strength and internal friction angle of grout-rock interface.

Moreover, it is noted that the cohesive strength and internal friction angle of samples before grouting are 31.05 kPa and 19.6°, i.e. they increased by 453.78% to 710.14%, and 64.85% to 112.81%, respectively, due to the injection of grout with W/C ration ranging from 1.5 to 0.8. Obviously, grouting is an effective method to improve the properties of samples.

Table 2. Results of the first set of tests.

Trial number	Shear strength (kPa)				Cohesive trength (kPa)	Internal friction angle (°)
	p = 100 kPa	p = 200 kPa	p = 300 kPa	p = 400 kPa		
Sample 1	346.58	425.26	510.45	615.32	251.55	41.71
Sample 2	301.65	366.5	440.37	534.53	217.74	37.69
Sample 3	241.83	388.4	552.93	752.17	171.95	32.31

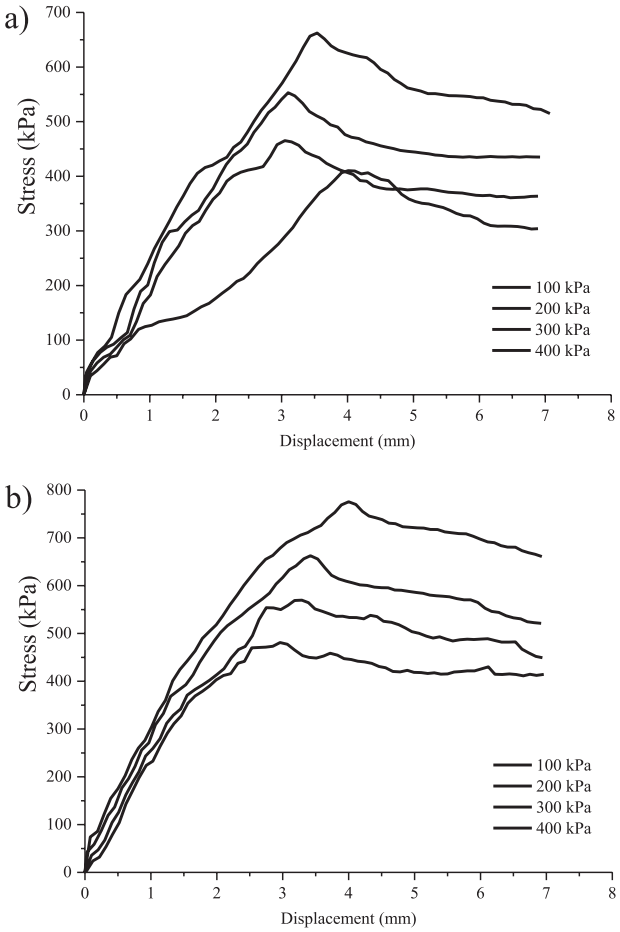

Fig. 7. Shear stress-strain curves of sample with different injection pressures.

Shear Properties of Grout-Rock Interface with Different Injection Pressures

Using the same method, the shear properties of grout-rock interface in different injection pressure conditions were also investigated. The shear stress-strain curves of samples with injection pressures of 1 MPa, 1.5 MPa and 2 MPa and a same W/C ratio of 1, are presented in Fig. 5b) (sample 2 and sample 4), Fig. 7a) (sample 5) and Fig. 7b) (sample 6), respectively.

Also, they all show significantly ductile behaviors in the shear process. First, the stress increases rapidly to a peak, and then gradually decreases to a stable value, as shown in Table 3. For example, as the vertical stress

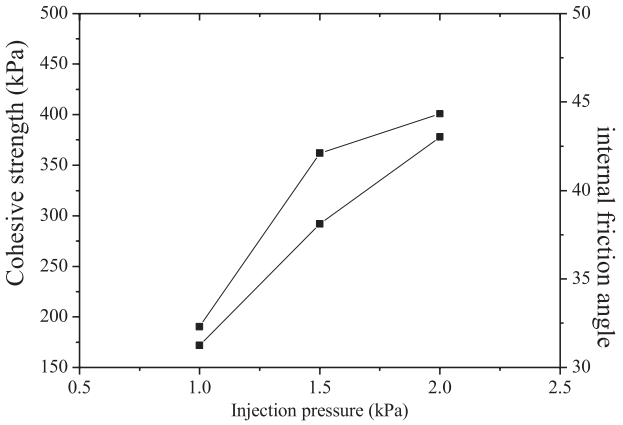

Fig. 8. Cohesive strength and internal friction angle of samples in different injection pressure conditions.

increases from 100 kPa to 400 kPa, the maximum stresses of sample 5 can increase by 18.73% ~ 19.80%, with the corresponding displacements ranging from 3.05×10^{-3} m to 4.31×10^{-3} m. While when injection pressure ranged from 1.5 MPa to 2 MPa, the maximum stresses of sample 6 can increase by 23.27 %, 22.28%, 19.84 % and 17.08%, respectively. Thus, higher injection pressure results in larger shear stress.

Based on the Mohr-coulomb law, the cohesive strength and internal friction angle of grout-rock interface in different injection pressure conditions were also acquired, as shown in Table 3. Hence, the direct shear strength of grout-rock interface with injection pressures of 1 MPa, 1.5 MPa and 2 MPa can be calculated with Eq. (4), Eq. (5) and Eq. (6), respectively.

$$\tau=0.77\sigma+217.74 \quad (4)$$

$$\tau=0.90\sigma+291.86 \quad (5)$$

$$\tau=0.98\sigma+377.98 \quad (6)$$

where, τ = shear strength of grout-rock interface, kPa; σ = vertical stress, kPa.

In addition, the influence of injection pressure on cohesive strength and internal friction angle were studied, as plotted in Fig. 8. It is obviously shown that higher injection pressure can result in larger cohesive strength and internal friction angle. Specifically, when

Table 3. Results of the second set of tests.

Trial number	Shear strength (kPa)				Cohesive strength (kPa)	Internal friction angle (°)
	p = 100 kPa	p = 200 kPa	p = 300 kPa	p = 400 kPa		
Sample 4	301.65	366.5	440.37	534.53	217.74	37.69
Sample 5	390.23	465.77	552.99	662.5	291.86	42.11
Sample 6	481.04	569.54	662.7	775.67	377.98	44.34

injection pressure ranged from 1 MPa to 1.5 MPa, the cohesive strength increases from 217.74 kPa to 291.86 kPa, and the internal friction angle rises from 37.69° to 42.11°. Furthermore, the cohesive strength and internal friction angle can increase by 29.51% and 5.30%, respectively, with injection pressure ranging from 1.5 MPa to 2 MPa. When injection pressure ranged from 1 MPa to 2 MPa, the cohesive strength and internal friction angle of samples after grouting can increased by 601.26% to 1117.33 %, and 92.30% to 126.22%, respectively. After that, conclusions can be drawn that not only cohesive strength but also internal friction angle can be increased due to the rise of injection pressure.

Conclusions

This paper aims at investigating on the shear properties of grout-rock interface by carrying out direct shear test. Based on the results obtained, the following conclusions can be made.

1. The gushed mud from fault-2 in Yonglian tunnel, which suffered multiple accidents such as collapse and mud inrush during the construction process, and a kind of Portland cement grout were selected as raw materials in this study. The raw materials are consistent with the engineering site, which increases the reliability of test results.

2. In order to simulate the actual generation environment of grout-rock interface, a test system consisting of cylindrical grouting device and parameter-controlled grout pumping equipment, was developed. This test system can realize the formation of grout-rock interface under high pressure conditions, which changes the situation that the previous study was carried out under no pressure.

3. Structural planes with a thickness of 1×10^{-3} m to 2×10^{-3} m were preseted inside the samples before grouting to get flatter grout-rock interfaces. However, there is no previous study on the properties of grout-rock interface. Therefore, it can be concluded that low W/C ratio and high injection pressure can significantly increase the cohesive strength and internal friction angle of grout-rock interface, which could aid in the design of grouting with this material in the future.

Acknowledgments

This study was funded by the National Natural Science Foundation of China (grant number 51909250), Shandong Natural Science Foundation (grant number ZR201807080053), Science and Technology Project of Housing Urban and Rural Construction in Shandong Province (grant number 2020-K4-2).

References

1. LI M.T., ZHANG X., KUANG W., ZHOU Z. Grouting reinforcement of shallow and small clearance tunnel. Polish Journal of Environmental Studies, **30** (1), 752, **2021**.
2. LIU J.G., ZHANG X., LI M.T., LAN X.D., HAO P.S. Research on permeation grouting mechanism considering gravity in the treatment of mud inrush disaster. Polish Journal of Environmental Studies, **30** (3), 2609, **2021**.
3. LI L.P., SHANG C.S., CHU K.W., ZHOU Z.Q., SONG S.G., LIU Z.H., CHEN Y.H. Large-scale geo-mechanical model tests for stability assessment of super-large cross-section tunnel. Tunnelling and Underground Space Technology, **109**, 103756, **2021**.
4. HEIDARI M., TONON F. Ground reaction curve for tunnels with jet grouting umbrellas considering jet grouting hardening. International Journal of Rock Mechanics & Mining Sciences, **76**, 200, **2015**.
5. SALIMIAN M.H., BAGHBANAN A., HASHEMOLHOSSEINI H. Effect of grouting on shear behavior of rock joint. International Journal of Rock Mechanics & Mining Sciences, **98**, 159, **2017**.
6. BEZUIJEN A., TE GROTENHUIS R., VAN TOL A.F., BOSCH J.W., HAASNOOT J.K. Analytical model for fracture grouting in sand. Journal of Geotechnical and Geoenvironmental Engineering, **137** (6), 611, **2010**.
7. FATTAH M.Y., AL-ANI M.M., AL-LAMY M.T.A. Studying collapse potential of gypseous soil treated by grouting. Soils & Foundations, **54** (3), 396, **2014**.
8. SONG B.D., PARK B.G., CHOI Y. Determining the engineering characteristics of the Hi-FA series of grout materials in an underwater condition. Construction & Building Materials, **144**, 74, **2017**.
9. LI P., ZHANG Q.S., LI S.C., ZHANG X. Time-dependent empirical model for fracture propagation in soil grouting. Tunnelling and Underground Space Technology, **94**, 103, **2019**.
10. VARGA D.L., MUÑOZ J.F., BENTZ D.P. Grout-concrete interface bond performance: Effect of interface moisture on the tensile bond strength and grout microstructure. Construction & Building Materials, **170**, 747, **2018.**
11. CHEN J., XU C. A study of the shear behavior of a Portland cement grout with the triaxial test. Construction & Building Materials, **176**, 81, **2018.**
12. JORNE F., HENRIQUES F.M.A. Evaluation of the grout injectability and types of resistance to grout flow. Construction & Building Materials, **122** (30), 171, **2016**.
13. LI S.C., SHA F., LIU R.T., ZHANG Q.S., LI Z.F. Investigation on fundamental properties of microfine cement and cement-slag grouts. Construction & Building Materials, **153**, 965, **2017**.
14. SHAHU J.T., PATEL S., SENAPATI A. Engineering properties of copper slag-fly ash-dolime mix and its utilization in the base course of flexible pavement. Journal of materials in civil engineering, **25**, 1871, **2013**.
15. YANG H.X. Experimental study on mechanical property of soil cement. 2nd international conference on electronic and mechanical engineering and information technology, 790, **2012**.
16. SULUGURU A.K., JAYATHEJA M., KAR A., GUHARAY A., SURANA A.R., JAMES N. Experimental studies on the microstructural, physical and chemical characteristics of building derived materials to assess their suitability in ground improvement. Construction & Building Materials, **156**, 921, **2017**.

17. HU W., SUI W.H., WANG D.L., MA L.X. Experimental investigation on mechanical properties and representative elementary volume for chemically grouted fractured rock masses. China Science Paper, **8** (5), 408, **2013**.
18. HAN L., ZONG Y., HAN G., ZHANG H. Study of shear properties of rock structural plane by grouting reinforcement. Rock and Soil Mechanics, **32**(9), 2570, **2011**.
19. ZHANG Q.S., LI P., ZHANG X., LI S.C., ZHANG W.J., LIU J.G., YU H.Y. Model test of grouting strengthening mechanism for fault gouge of tunnel. Chinese Journal of Rock Mechanics & Engineering, **34** (5), 924, **2015**.
20. LI P., ZHANG Q.S., ZHANG X., LI S.C., LI X.H., ZUO J.X. Grouting Diffusion Characteristics in Faults Considering the Interaction of Multiple Grouting. International Journal of Geomechanics, **17** (5), 1, **2016**.
21. ZHANG Q.S., LI P., WANG G., LI S.C., ZHANG X., ZHANG Q.Q., WANG Q., LIU J.G. Parameters Optimization of Curtain Grouting Reinforcement Cycle in Yonglian Tunnel and Its Application. Mathematical Problems in Engineering, **12**, 2, **2015**.
22. LI P., ZHANG Q.S., ZHANG X., LI S.C., ZHANG W.J., LI M.T., WANG Q. Analysis of fracture grouting mechanism based on model test. Rock and Soil Mechanics, **35**(11), 3221, **2014**.
23. CHUN B.S., YONG J.L., CHUNG H.I. Effectiveness of leakage control after application of permeation grouting to earth fill dam. KSCE Journal of Civil Engineering, **10**(6), 405, **2006**.
24. GOTHÄLL R., STILLE B. Fracture-fracture interaction during grouting. Tunnelling and Underground Space Technology, **25**(3), 199, **2010**.
25. YUN J.W., PARK J.J., KWON Y.S. Cement-based Fracture Grouting Phenomenon of Weathered Granite Soil. KSCE Journal of Civil Engineering, **21**(1), 1, **2016**.
26. CHEN J.H., HAGAN P., SAYDAM S. Shear behavior of a cement grout tested in the direct shear test. Construction & Building Materials, **166**, 271, **2018**.